View metadata, citation and similar papers at core.ac.uk
brought to you by CORE
provided by NASA Technical Reports Server

NASA-CR-198859

IN-76-CR
OCIT.
56854
p. 20

DIAMOND THIN FILM TEMPERATURE AND HEAT-FLUX SENSORS

M. Aslam, G. S. Yang, A. Masood and R. Fredricks
Department of Electrical Engineering
Michigan State University
East Lansing, MI

Grant NAG-1-1328
July 3, 1995

National Aeronautics and Space Administration
Langley Research Center
Hampton, Virginia 23681-0001

(NASA-CR-198859) DIAMOND THIN FILM TEMPERATURE AND HEAT-FLUX SENSORS Final Report (Michigan State Univ.) 20 p

N95-30847

Unclas

G3/76 0056854

Table of Contents

Section			Page
ABSTRACT			i
I.	INTRODUCTION		1
II.	SENSOR INFRA-STRUCTURE		2
	II.1	Diamond Film Growth	2
	II.2	Nucleation, Patterning and Doping	2
	II.3	Metallization and Electronic Properties	3
	II.4	Reliability	4
III.	SENSOR TEST CHIPS		5
	III.1	1st Generation Test Chip	5
		III.1.1 Temperature Sensors	6
		III.1.2 Heat Flux Sensors	7
		III.1.3 Problems	10
	III.2	2nd Generation Test Chip	10
		III.2.1 Ultra-High Nucleation Density Technique	11
		III.2.2 Thermistor Response	13
	III.3	3rd Generation Test Chip	14
IV.	3-D DIRECT-WRITE PATTERNING SYSTEM		14
V.	CONCLUSIONS		15
VI.	REFERENCES		16

Abstract

Diamond film temperature and heat-flux sensors are developed using a technology compatible with silicon integrated circuit processing. The technology involves diamond nucleation, patterning, doping and metallization. Multi-sensor test chips were designed and fabricated to study the thermistor behavior. The minimum feature size (device width) for 1st and 2nd generation chips are 160 and 5 μm, respectively. The p-type diamond thermistors on the 1st generation test chip show temperature and response time ranges of 80-1270 K and 0.29-25 μs, respectively. An array of diamond thermistors, acting as heat flux sensors, was successfully fabricated on an oxidized Si rod with a diameter of 1 cm. Some problems were encountered in the patterning of the Pt/Ti ohmic contacts on the rod, due mainly to the surface roughness of the diamond film. The use of thermistors with a minimum width of 5 μm (to improve the spatial resolution of measurement) resulted in lithographic problems related to surface roughness of diamond films. We improved the mean surface roughness from 124 nm to 30 nm by using an ultra high nucleation density of 10^{11} cm^{-2}. To deposit thermistors with such small dimensions on a curved surface, a new 3-D diamond patterning technique is currently under development. This involves writing a diamond seed pattern directly on the curved surface by a computer-controlled nozzle.

I INTRODUCTION

Common types of temperature sensors [1,2,3] are thermocouples, resistance temperature detectors (RTD), thermistors, integrated circuit (IC) sensors, diodes and transistors. Thermocouples [4] offer the largest range (33 to 2573 K) and linear response but are the least sensitive. RTDs [5] show poor sensitivity and limited range (33 to 923 K). The thermistors [6,7,8] with a reported range of 173 to 1173 K are very sensitive but nonlinear. The IC sensors offer a short range (223 to 408 K), a good linearity and high sensitivity. The reported response times for various types of temperature sensors are in the range of fraction of a second to few hundred seconds. These sensors fail or show poor sensitivity and response in harsh environments such as those prevailing in aerospace systems. New material technologies are, therefore, needed for temperature sensors with high sensitivity, large temperature range, fast response time, and high resistance to harsh environments (mechanical, chemical and radiation).

Due to a unique combination of its mechanical, electrical, thermal and chemical properties, diamond is an excellent material for temperature and heat flux sensors. Although natural and synthetic diamond thermistors [9] were demonstrated for temperatures below 600 K already in the sixties, they were never commercialized due mainly to high cost. Recently, there has been a renewed interest in diamond thermistors [10] because of a rapid progress in diamond film fabrication using the chemical vapor deposition (CVD) process which can produce inexpensive polycrystalline diamond films on non-diamond substrates such as Si. In the past several years, Michigan State University has provided leadership in the development of diamond-based sensors and micro-machining [11,12,13] (Fig. 1). The goals of the research effort are to develop (i) diamond sensors for temperature, pressure and acceleration, and (ii) diamond field emitters for flat panel displays and pressure sensors. The research approach consists of (a) study of fundamental concepts, (b) development of materials technology and (c) fabrication of prototypes.

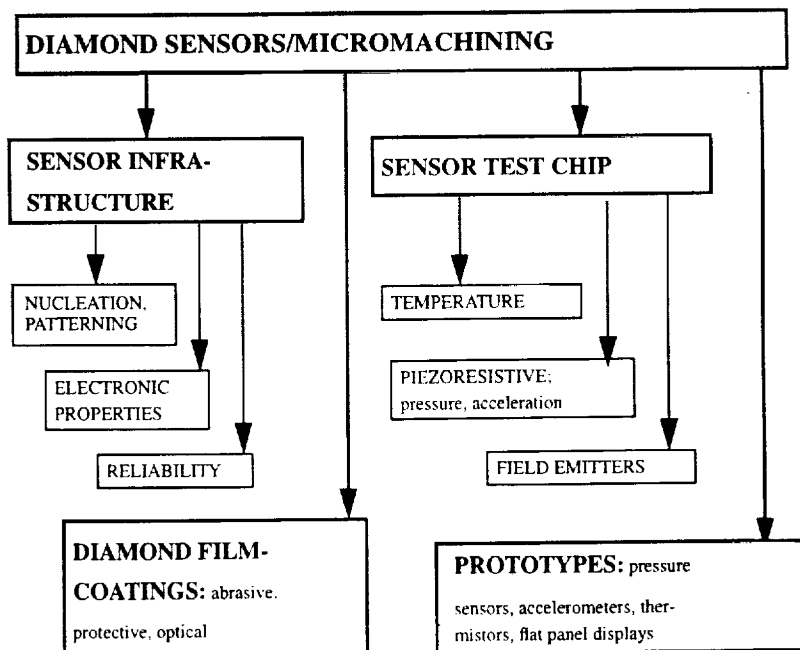

Fig. 1 Sensor research at Michigan State University.

A 1st generation test chip containing diamond thermistors [12] with a minimum device width of 160 μm, developed for NASA Langley, showed high sensitivity in the temperature range of 80 - 1270 K in vacuum. The response times at 300 K were 25 μs (measured) and 290 ns (calculated) for silicon and SiO_2 substrates, respectively. In a further study, a 2nd generation multi-sensor test chip was developed. The minimum thermistor width on the chip is 5 μm. A new 3-D patterning technique is being developed to transfer such small feature sizes on a curved surface. This report describes the work done for NASA Langley. In particular, (a) diamond sensor infra-structure, (b) design, fabrication and testing of a flat multi-sensor test chip, and (c) heat flux sensors on flat and curved substrates will be discussed.

II SENSOR INFRA-STRUCTURE

To develop reproducible and reliable diamond micro-sensors and field emitters [13,14], it was necessary to develop sensor infrastructure. The infrastructure development, compatible with Si integrated circuit technology, includes diamond film growth, nucleation, patterning, doping, metallization, electronic properties and reliability which are described in this section:

II.1 Diamond Film Growth

High quality p-type polycrystalline diamond films were deposited on oxidized Si substrates using hot filament CVD [15,16]. The filament and substrate temperatures were 2073 - 2473 and 1073 - 1273 K, respectively. The gases used for film growth consisted of either hydrogen with 1% C_2H_2 and 0.5% CO or hydrogen with 1% CH_4. The deposition pressure, growth rate and film thickness were typically in the range of 50 - 70 torr, 0.15 - 0.5 μm per hour and 1.5 - 6 μm, respectively. The film quality was monitored by Raman spectroscopy, scanning electron microscopy (SEM), and atomic force microscopy (AFM).

II.2 Nucleation, Patterning and Doping

For diamond growth on non-diamond substrates, the substrate surface is treated, usually with diamond powder, to enhance the nucleation density. The conventional diamond film nucleation and patterning techniques require some treatment of the substrate surface which normally causes a surface damage [17,18,19,20]. Our nucleation and patterning techniques [21,22] do not damage the surface and are IC-compatible.

In our techniques, diamond powders with mean sizes of 0.038 or 0.101 μm are suspended into carrier fluids to prepare the so called diamond powder loaded fluid (DPLF). As shown in Fig.2, the DPLF is coated on an oxidized Si wafer and then patterned using standard photolithography. The sample is subsequently placed in the diamond deposition reactor and the carrier materials evaporate at 1163 K leaving behind the diamond powder particles which act as

seeds for diamond growth. The techniques can be used to grow polycrystalline films on a variety of substrates of different shapes, and can be used for mechanical and optical coatings. It is amenable to ultrahigh nucleation density (above 10^{11} cm^{-2}) and low temperature (~743 K) diamond growth [23].

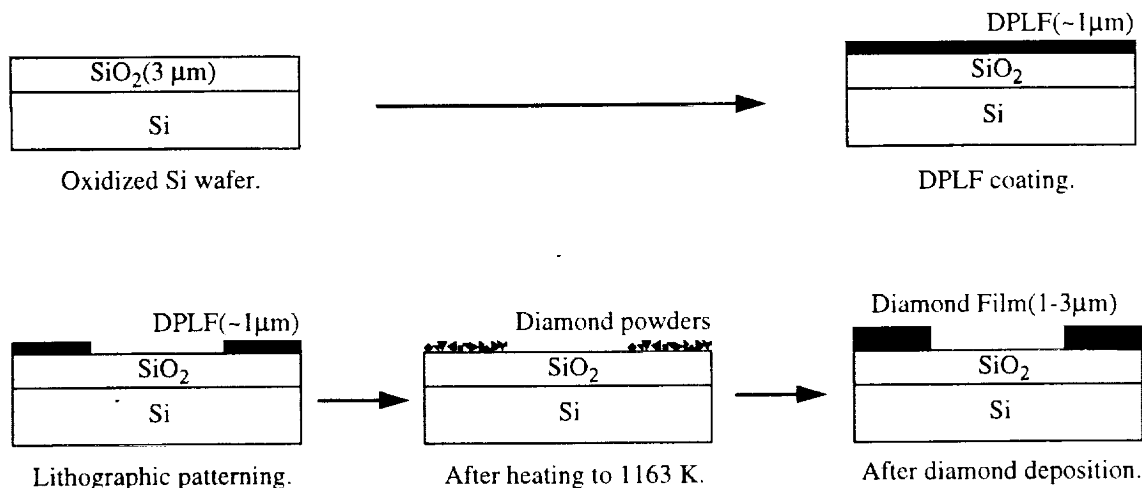

Fig. 2 Patterning of diamond film by DPLF method (not to scale).

The films were doped p-type during the growth process, as described in section II-1, using pure boron powder which was placed in a holder on the substrate heater plate near the substrate so that the holder temperature was close to 1163 K. Electronic properties of the p-type films are described in the next section.

II.3 Metallization and Electronic Properties

Most of the earlier metallization studies [24,25,26,27] focused on ohmic contacts on polycrystalline and single crystal diamond. As our aim was to fabricate diamond sensors, the choice of contact metal was based on (i) ohmic contacts, (ii) good adhesion to both diamond and silicon dioxide and (iii) resistance to high temperatures (up to 1273 K). A double-layer structure consisting of Pt on Ti was selected. Ti makes ohmic contacts with diamond [28,29] and provides a good adhesion between diamond and SiO_2, whereas Pt is resistant to oxidizing ambients. An anneal for 30 min at 923 K in vacuum (10^{-7} torr) resulted in stable and reproducible contacts. It is believed that, during this anneal, Ti reacts with diamond to make its carbide [30] and it reacts with Pt to make its alloys [31] which are stable at 1273 K. The quality of diamond, monitored through SEM and Raman, was not affected by this anneal. For low temperature applications, Al or Cr are used as contact metals.

Hall mobility, hole concentration and resistivity were measured for different doping levels and at various temperatures. The Hall mobility and resistivity ρ are in the ranges of 2 - 50 $cm^2V^{-1}s^{-1}$ and 0.2 - 70 Ω-cm, respectively [12]. The activation energies for boron, computed from the slopes of measured ρ versus 1/T curves assuming no compensation, are in the range of 0.22 - 0.34 eV for the unannealed samples. These values correspond to hole concentration values in the range of 10^{18} - 2.0 x 10^{15} cm^{-3}.

II.4 Reliability

The effect of high temperature annealing on the film quality was studied to make reliable and reproducible sensors. We find that, for p-type diamond films, the resistivity decreases for vacuum anneal above 573 K. However, in case of undoped films, annealing above 573 K causes an increase in resistivity [32] which may be related to hydrogen out-diffusion. From a detailed study of the annealing behavior, we concluded that an anneal for 8 min at 1273 K in vacuum (10^{-7} torr) makes the temperature behavior very stable for temperature measurement in the range of 80 to 1273 K if the measurement is done in vacuum. The annealing time needed to stabilize the resistivity at 1273 K seems to be independent of doping level. The quality of diamond, monitored through SEM and Raman, was not affected by the vacuum anneal at 1273 K. However, heating of films to 1273 K for 2 minutes at a pressure of 100 mtorr resulted in a significant amount of erosion of the film. This may be due to oxidation of diamond caused by residual water vapors present at 100 mtorr. In our earlier experiments, diamond films were found to oxidize in pure oxygen at temperatures > 923 K. Fig. 3 shows etched thickness against etching time of diamond films at 973 K under flowing oxygen of 40 sccm. For the linear part of the curve, the etch rate was computed to be ~ 5 nm/sec. Oxidation of diamond by oxygen plasma was observed even at lower

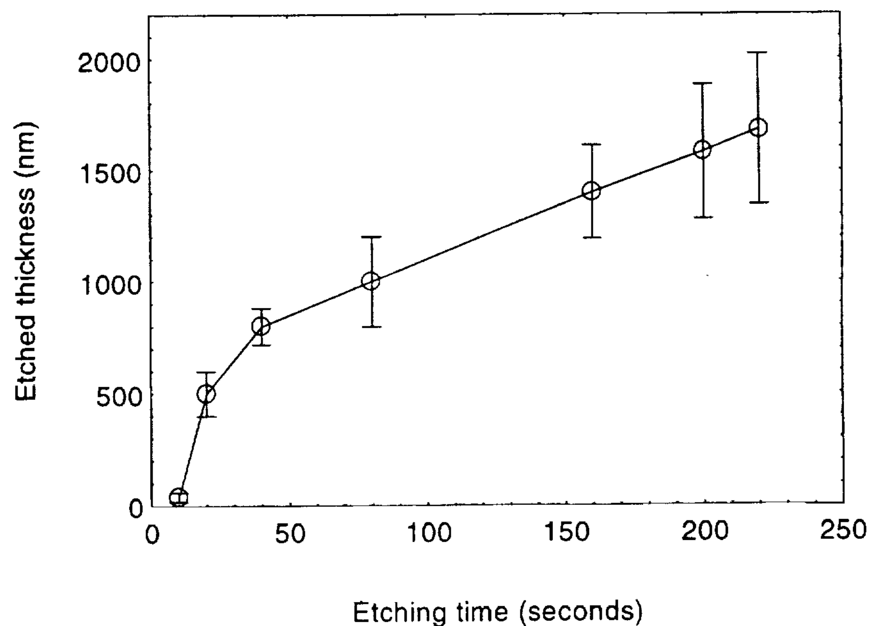

Fig. 3 Etching of diamond films in a rapid thermal processor at 973 K under an oxygen flow of 40 sccm.

temperatures [33]. Thus, in an oxygen ambient, the thermistor is stable only below 923 K. The use of thermistor in an oxidizing ambients at high temperatures may be possible if the diamond film is passivated for example with SiO_2 or Si_3N_4, which may, however, increase the response time of the thermistor.

III SENSOR TEST CHIPS

To study the electronic and sensing properties of CVD diamond, and to fabricate prototype sensors, 1st and 2nd generation sensor test-chips were developed. The 1st generation test chip was used solely for NASA research. The 2nd generation chip was used for NASA research as well as for research on piezoresistive sensors [11].

The 1st generation test chip, with a chip size of 1 x 1 cm^2 and minimum diamond device width of 160 μm, contains thermistors, Hall Van der Pauw structure and a metal-oxide-semiconductor field effect transistor (MOSFET). The 2nd generation test chip was used to study the fabrication technology of very small size thermistors. This test chip, in addition to structures found on the 1st generation chip, contains a pressure sensor, an accelerometer, a Hall sensor and cantilever beams. It has a minimum diamond feature size (thermistor width) of 5 μm. A six-mask process is employed for its fabrication using four-inch Si wafers as substrates. The results reported in this section deal with the test chips.

III.1 1st Generation Test Chip

The first generation diamond test chip (Fig. 4) was primarily designed for the study of thermistors. This study led to the technology of heat flux gauges on oxidized Si rods with a diameter of 1 cm. The chip uses 500 μm thick oxidized Si wafer as the substrate material. The thermistors consist of p-type polycrystalline diamond films with a thickness in the range of 4 - 6 μm. The metal contacts consist of Pt/Ti double layer whereby Ti enhances adhesion between Pt and diamond.

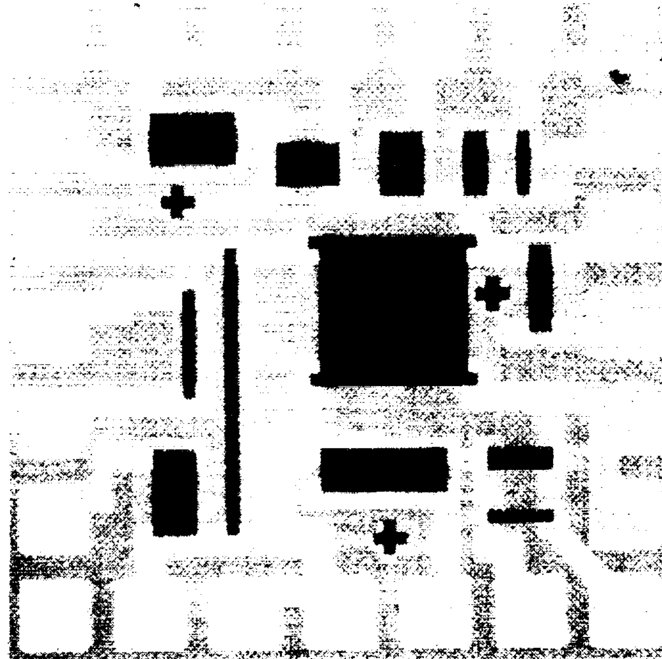

Fig. 4 First generation diamond test chip.

III.1.1 Temperature Sensors

The resistivity measured as a function of temperature, for the thermistors on the 1st generation chip with three different hole concentration levels, is shown in Fig. 5(a). All the samples were annealed at 873 K and 1273 K for 35 and 8 minutes, respectively, at a pressure of 10^{-7} torr before the measurements. The temperature response was measured over the temperature range of 80 - 1273 K and found reproducible for a number of temperature cycles of less than 1 minute duration. The thermistors have a negative temperature coefficient (NTC) of resistance over the entire range. As shown in Fig. 5(b), the $\Delta\rho/\Delta T$ values computed from the curves shown in Fig. 5(a) are in the ranges of 5.0×10^{-7} - 7.0×10^{-3}, 6.0×10^{-6} - 1 and 6.0×10^{-6} - 2 Ω-cm/K for the hole concentrations of 9.6×10^{18}, 1.72×10^{16} and 2×10^{15} cm^{-3}, respectively.

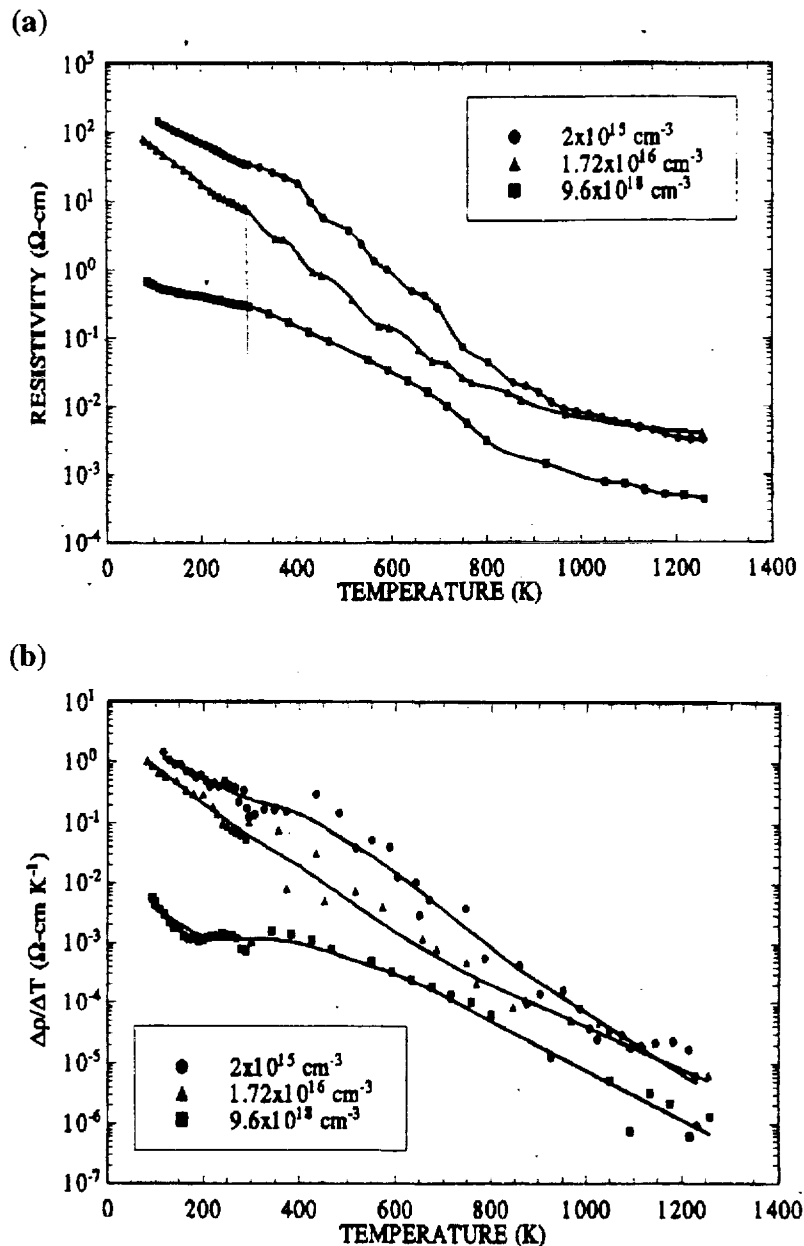

Fig. 5 The resistivity ρ and $\Delta\rho/\Delta T$ ploted as funtion of temperature for samples with three different hole concentration.

The temperature coefficient α, defined by $\alpha = \rho^{-1}\Delta\rho/\Delta T$, is in the range of -0.005 to -0.02 K^{-1} for the measured temperature range and for the above hole concentration values. As the average value [3] of α for Pt RTD is 0.003853 K^{-1}, the sensitivity of diamond sensors is better than that of Pt RTD over

most of the temperature range. However, most thermistors show a typical value of α in the range of 0.2 - 0.4 but over a limited temperature range, typically 100 K [3]. Although, α is widely used to represent the sensitivity of temperature sensors, it was basically devised for RTDs and is not suitable for comparison of sensitivity for semiconductor sensors. For example, a 100 KΩ thermistor and a 25 Ω RTD, both with $\alpha = 0.001$ and temperature change of 1 K, will show resistance changes of 100 Ω and 25 mΩ, respectively. The change of 100 Ω is readily measurable while the change of 25 mΩ requires precision test equipment. Thus, the best measure for diamond thermistors is $\Delta\rho/\Delta T$.

The dynamic thermal response time of thermistors on the 1st generation chip, measured by applying a square wave current pulse to the sensor, was found to be 25 µs. This is a fairly small time constant as compared to commercial temperature sensing devices [3] with time constant in the range of milliseconds to several tens of seconds. To achieve fast response, sensors are usually mounted on thermal insulators such as Al_2O_3 or fused quartz [34]. As in our case the sensor is separated from the 500 µm thick Si substrate only by a 2 µm thick layer of SiO_2, the response time of 25 µs is expected to be dominated by the thermal properties of Si. The time constant can be computed for a SiO_2 substrate using the thermal properties of Si and SiO_2. Such a computation predicts a time constant of 0.29 µs for a diamond sensor directly on the SiO_2 substrate. This value may be reduced further (i) by reducing the thermal mass of the sensor and/or (ii) through use of micro-machining to fabricate a free standing sensor element.

III.1.2 Heat Flux Sensors

After an intensive study of diamond temperature sensors, arrays of diamond heat flux sensors were fabricated on (i) a 2 x 3 cm^2 flat oxidized Si wafer and (ii) an oxidized Si rod with a length of 7.6 cm and a diameter of 1 cm. The flat sample (sensor test chip) was used to study the uniformity of doping level and difference in temperature response of individual thermistors. This sample was sent to NASA after initial testing at Michigan State. The cylindrical substrate is considered for possible measurement of heat flux in wind tunnels.

The flat sensor test chip consists of an array of ten thermistors with dimensions of 250 x 800 μm^2 with center to center spacing of 400 µm. A schematic diagram of thermistor array is shown in Fig. 6 and measurement data is listed in Table 1. The non-uniformity in film thickness was within 4%. A variation of 7% in the width of thermistors was introduced due to the use of transparency type masks. The resistivity was measured as a function of temperature in the range of 300 - 673 K for selected thermistors. The temperature response for each thermistor was stable and repeatable after an anneal for 10 min at 673 K. Fig. 7(a) shows the resistivity as a function of temperature for selected diamond thermistors. A large variation in the initial resistivity values for thermistors fabricated at the same run was observed. It is believed to be due to the nonuniform

doping. The percentage change of resistivity at different temperatures was found to be consistent for all thermistors fabricated in the same run despite the large variation in initial resistivity values. The temperature dependence of normalized resistivity (R_T/R_{To}) for all thermistors is shown in Fig. 7(b). The temperature range of these thermistor is limited to 673 K because Al was used as a metal contact.

Fig. 6 The schematic diagram of an array of diamond heat flux sensors. The chip size is 2 x 3 cm^2.

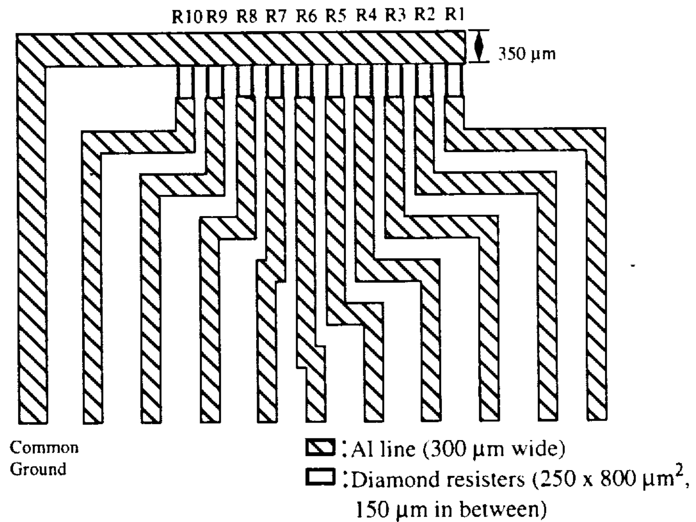

Table 1: The measurement data for 6 resistors of Fig. 6.

	R1	R3	R4	R6	R9	R10
Thickness (μm)	1.23	1.19	1.23	1.19	1.19	1.18
Width (μm)	267	260	272	253	261	256
Length (μm)	225	235	235	250	240	235
R (kΩ at 23°C)	85.5	88.9	319.2	440.7	532.5	509.5

For the fabrication of diamond thermistors on the rod, standard lithographic procedures were modified to accomplish patterning on a curved surface. Employing high quality transparency type (flexible) masks, a patterned diamond seed layer was applied to rod surface using the procedure depicted in Fig.2. The deposition of patterned diamond thermistors was successfully completed. An array of 12 diamond thermistors with dimensions of 150 X 2000 μm was fabricated over a small region (~35°) on the rod as shown in Fig. 8. For the electrical contacts to the thermistors, a Pt/Ti double layer was used. The problems encountered in patterning the Pt/Ti

contacts were mainly related the etching of Pt/Ti.

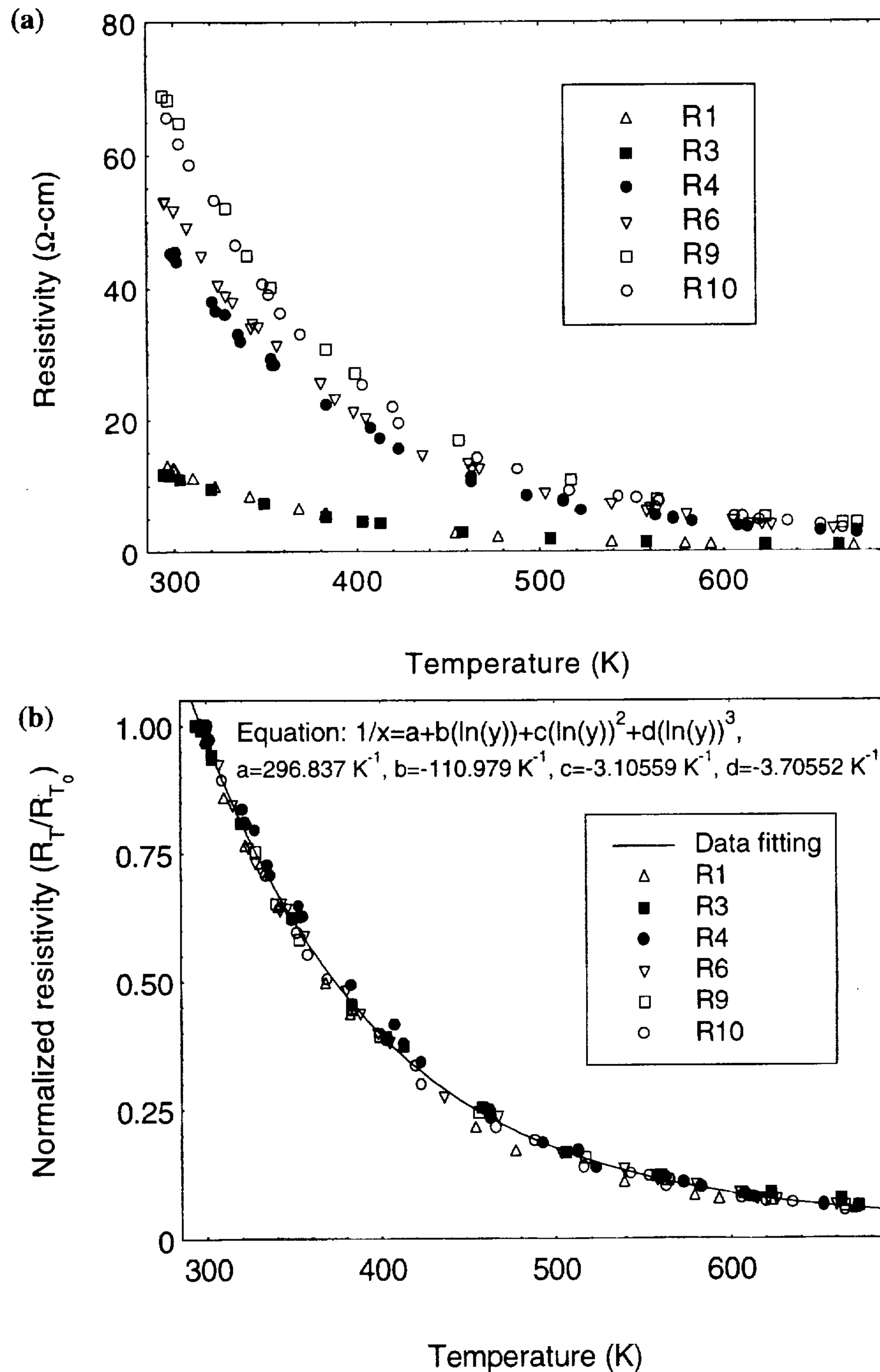

Fig. 7 The resistivity (a) and normalized resistivity (b) versus temperature for selected diamond thermistors. (T_0 = 300 K)

III.1.3 Problems

The technology developed for the 1st generation diamond test chip demonstrated successfully the excellent sensing properties of diamond thermistors. However, this also revealed some problems related to small feature sizes, 3-D patterning and metal contacts. The surface roughness of diamond films used in the first generation test chip was in the range of 0.5 -2 μm depending upon the film thickness. This results mainly from polycrystalline nature of the films and the low diamond nucleation density which is in the range of 10^8 cm^{-3}. Due to the roughness; (i) the targeted dimensions of small feature sizes were difficult to achieve, (ii) problems were encountered in post-deposition lithography, and (iii) the etching of metal contacts was complicated. To study such problems, a 2nd generation test chip was designed, fabricated and tested. A new 3-D patterning techniques was developed to overcome the problems associated with diamond film patterning on curved surfaces.

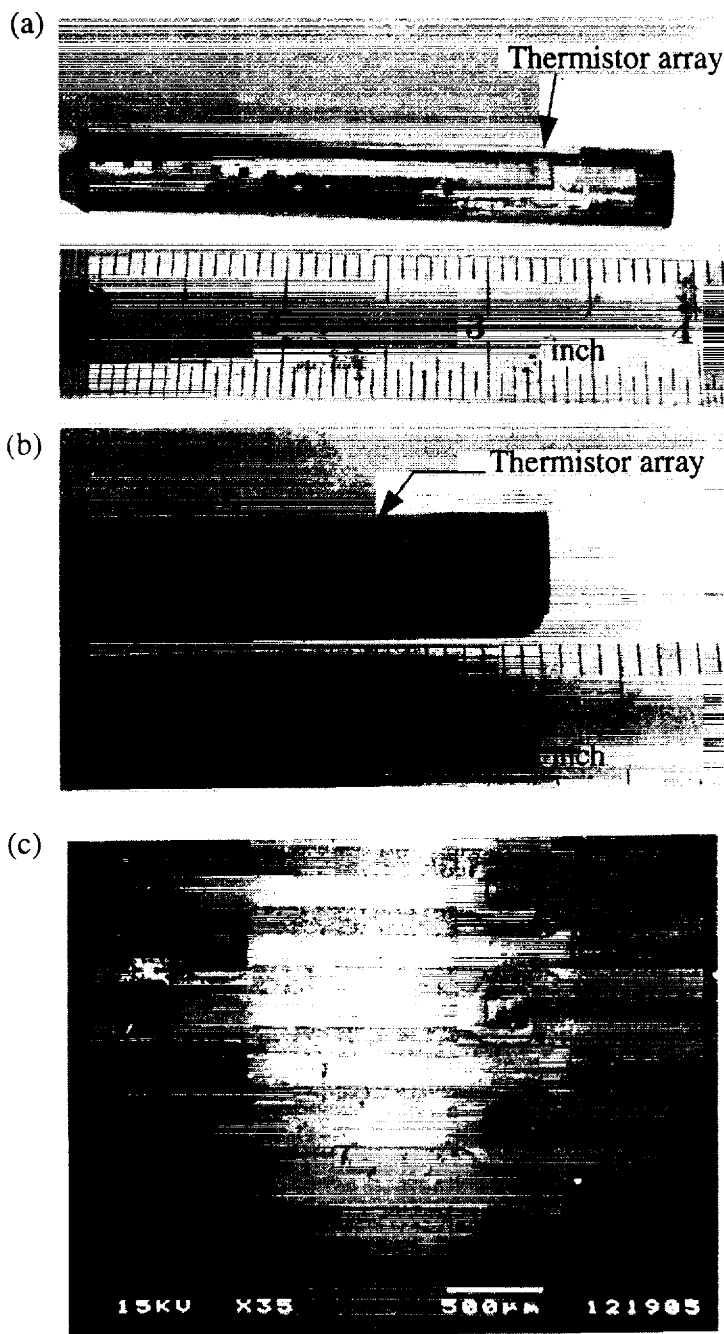

Fig. 8 Pictures of diamond thermistors on the Si rod (a-c).

III.2 2nd Generation Test Chip

A second generation test chip, with a minimum feature size of 5 μm, was developed. It has a variety of test structures including thermistors, a pressure sensor, an accelerometer, a magnetic field sensor and a metal-oxide-semiconductor field effect transistor (MOSFET). Fig. 9 shows an overview of this chip. The chip was used to study the surface roughness and thermistor response.

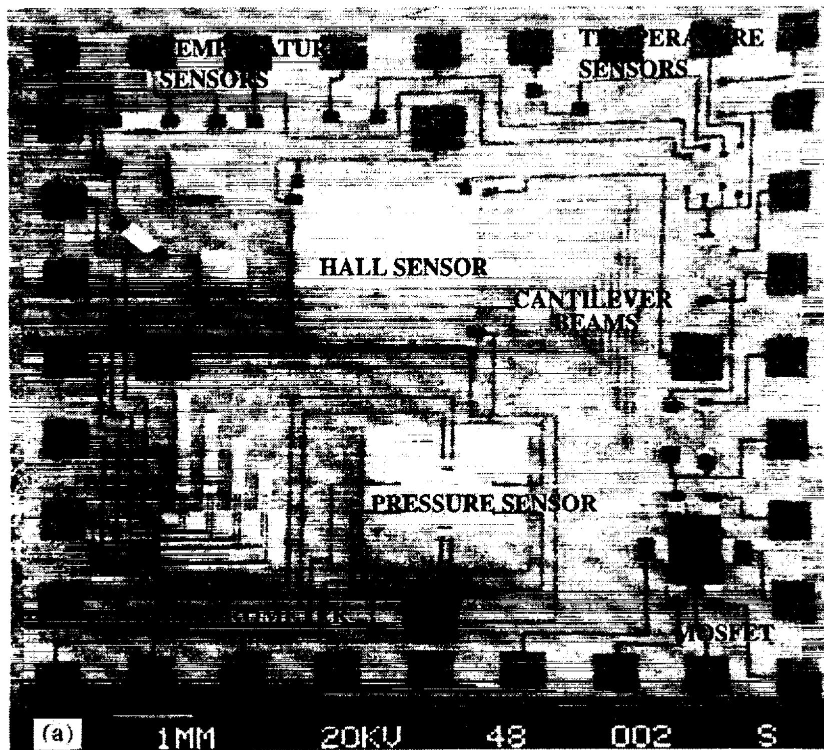

Fig. 9 Overview of 2nd generation test chip.

III.2.1 Ultra-High Nucleation Density Technique

To address the problems associated with the surface roughness, an ultrahigh density seeding technique was developed enhancing the nucleation density to 10^{11} cm^{-2} [22,35]. Diamond powder with a particle size of 0.038 μm was used to achieve this. A comparison of this technique with the low nucleation density techniques, used for 1st generation test chip, is provided in Table 2.

Table 2: Technical details of low and ultrahigh nucleation densities techniques.

	Low Density	Ultrahigh Density
Carrier Fluid	Photoresist	Water
Powder Size	0.101 μm	0.038 μm
Density	12 carats/liter	40 carats/liter
Nucleation Density	~ 10^8 cm^{-2}	~ 10^{11} cm^{-2}
Application Methods	Spray, Spin	Spray, Brushing, Direct Writing
Patterning	Photolithography	Photolithography, Direct Writing

The ultrahigh nucleation density tremendously reduces the deposition time even for the low temperature (673 - 773 K) deposition, which in general has a low deposition rate of approximately 0.05 μm per hour [23,36]. Very smooth film surfaces were observed as a result of ultrahigh nucleation density. In order to compare the surface roughness of films with the same thickness, two sets of samples were prepared by hot filament CVD for low and ultrahigh seeding densities. Fig. 10 shows atomic force microscopy (AFM) surface plots of 1 micron thick films

seeded by nucleation densities of $\sim 10^{8}$ cm^{-2} and $\sim 10^{11}$ cm^{-2}.The average surface roughness for

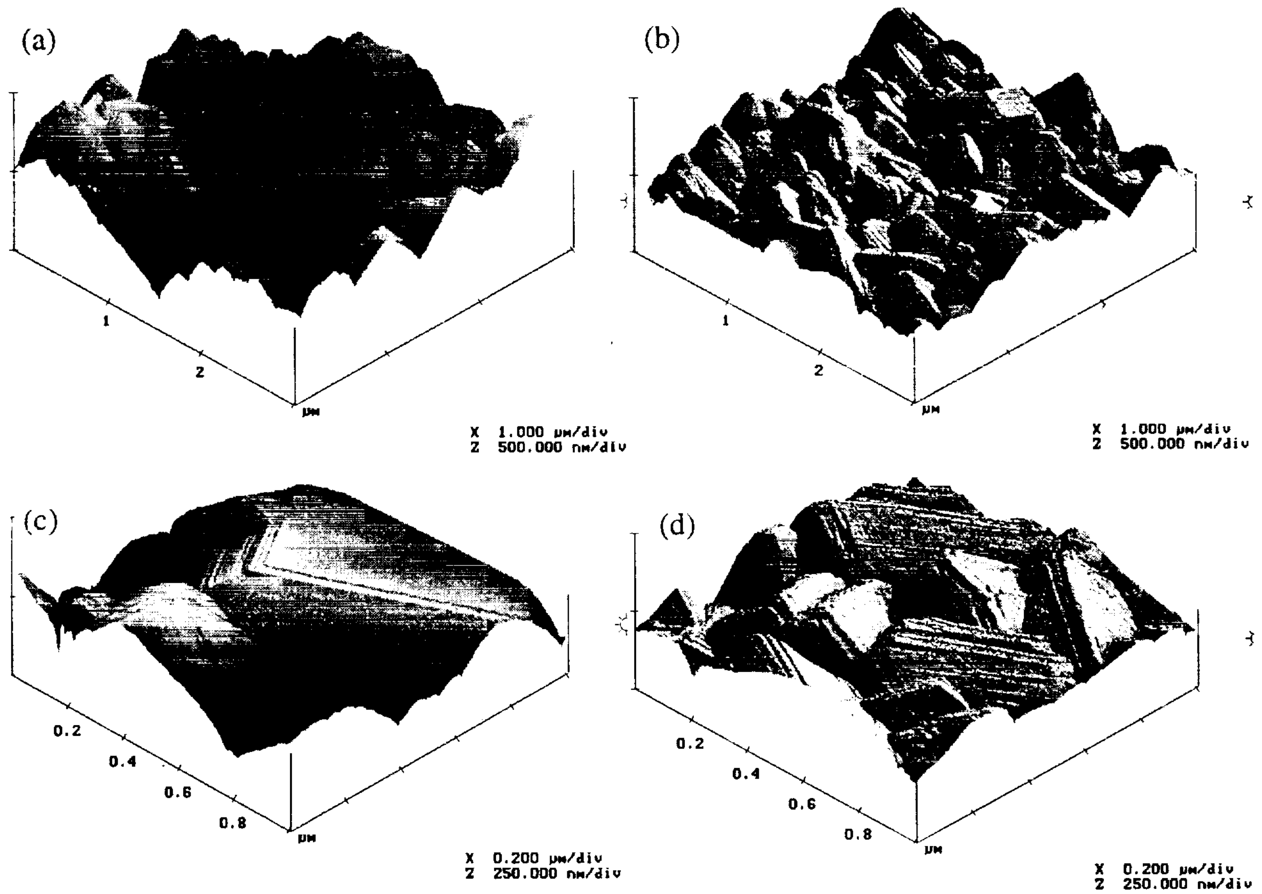

Fig. 10 Atomic force microscopy micrographs of 1 µm thickness films for low (a, c) and ultrahigh (b, d) nucleation densities.

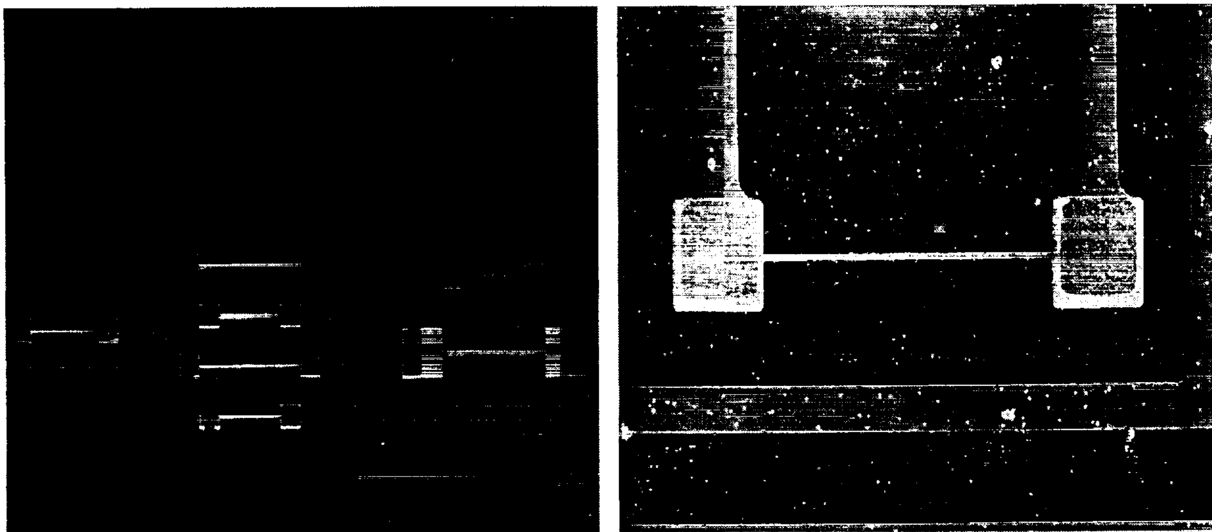

Fig. 11 Pictures of thermistors (a) used for temperature response, and close-up view of 5 µm wide thermistor (b).

the ultrahigh density is approximately 30 nm as compared to 124 nm for the low density [35].

III.2.2 Thermistor Response

The resistors used for the temperature sensing properties are shown in Fig. 11 which also shows a close-up view of the thermistor with a feature size of 5 μm in width. The thermistor response is shown in Fig. 12 and the film properties are summarized in Table 3.

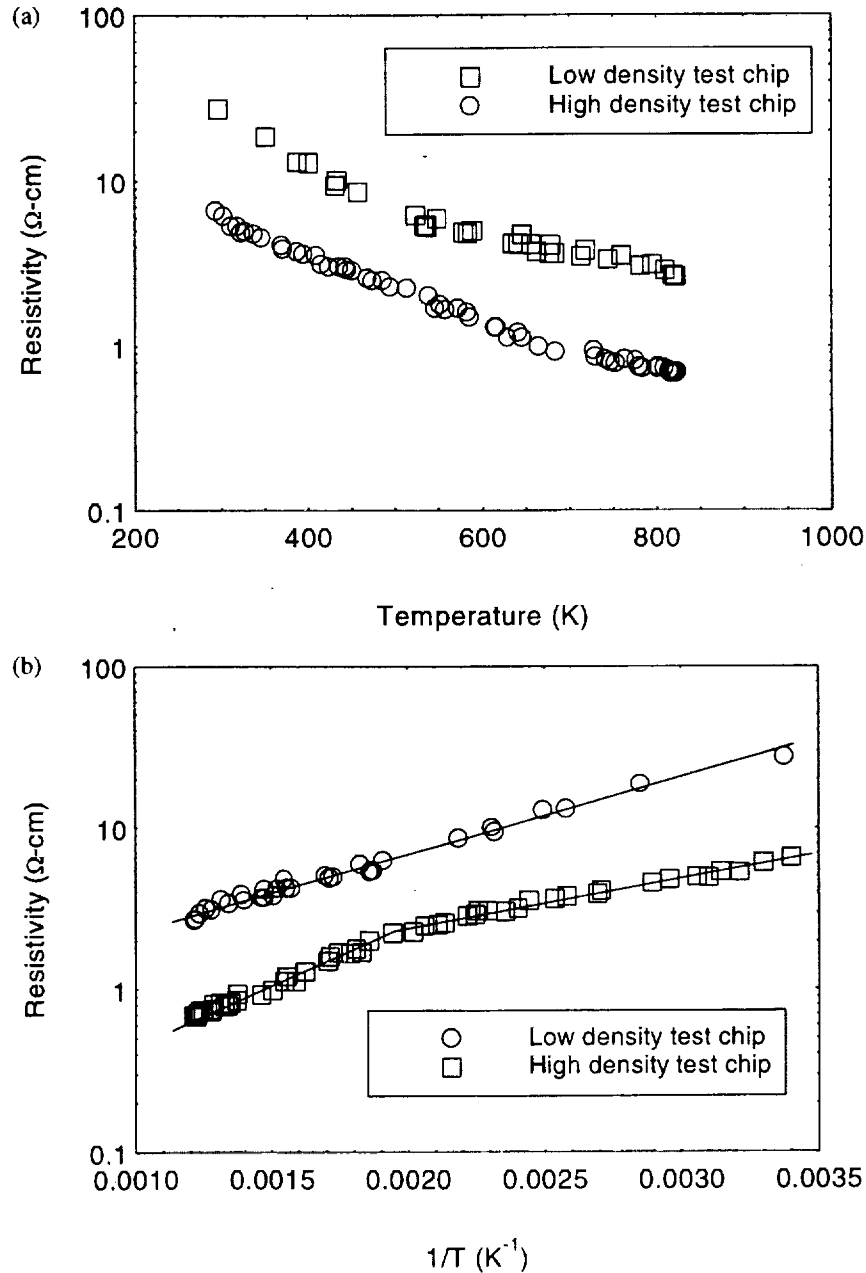

Fig. 12 The temperature response of resistivity for both high and low nucleation density samples.

The Hall mobility and concentration are measured by Hall Van der Pauw method [37]. The temperature response of resistivity for both low and ultrahigh nucleation densities samples was measured in the temperature range of 300 - 825 K. As seen in Fig. 12 (b), the two straight lines with different slopes intersected at a temperature of 525 K for the ultrahigh density sample. It suggests two activation energies for boron in highly doped diamond within this temperature range. The high density sample has a lower resistivity and higher Hall concentration than low density one. The larger amount of grain boundaries, which contain more dopant impurities and defects, present in high nucleation density samples is believed to contribute to the higher conduction of high-density samples.

Table 3: The characteristic of films seeded by low and ultrahigh densities.

	Low Density	Ultrahigh Density
Nucleation Density (cm^{-2})	~ 10^8	~10^{11}
Average Surface Roughness (nm)	124	30
Maximum Roughness (nm)	888	264
Resistivity (Ω-cm)	27.0538	6.9461
Hall Mobility (cm^2/V-s)	0.9141	1.0938
Hall Concentration (cm^{-3})	2.5273 x 10^{17}	8.226 x 10^{17}

III.3 3rd Generation Test Chip

The design of 3rd generation test chip focuses on (i) small feature sizes (1-2 μm), (ii) free standing thermistor structures to enhance response time and (iii) mass air flow sensors. The small feature size will permit high resolution of temperature variations. For the operation of diamond thermistors in oxidizing environments, a passivation layer (SiO_2 or Si_3N_4) is required to prevent diamond from oxidation at a temperature higher than 873 K. However, the passivation layer may increase the response time. In order to improve the sensor's response time, a free standing structure is useful to minimize the amount of heat dispensed into the substrate. These and other issues are currently addressed in the design of third generation test chip.

IV 3-D DIRECT-WRITE PATTERNING SYSTEM

In spite of its many advantages, the patterning technique currently employed in our sensor fabrication processes is limited to flat substrates. Additionally, as shown in Fig. 11 (a) and (b), the stray diamond particles with a density of ~10^5 cm^{-2} appear in non-diamond areas. They cause a serious problem if thick diamond films are grown. A new patterning technique for CVD diamond

is currently under development to achieve both arbitrary shaped and highly selective diamond patterning. In this technique, diamond seed patterns are directly written on a substrate [38] using fine nozzles. A schematic diagram is shown in Fig. 13. Computer controlled 3-dimensional position stages coupled with nozzles are used to write patterns on a substrate. Such a direct-write system is currently under construction. The system is expected to help produce heat flux sensors on curved substrates.

Fig. 13 Schematic diagram of direct-write diamond seeding system.

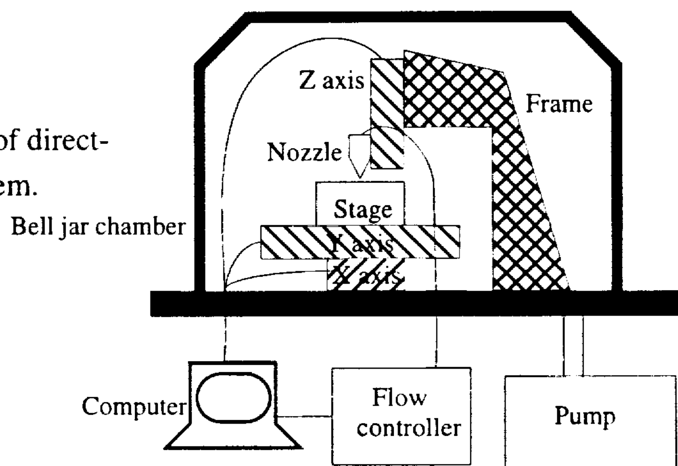

V CONCLUDSIONS

Boron-doped CVD diamond thermistors show temperature and response time ranges of 80 - 1270 K and 0.29 - 25 μs, respectively. The use of thermistors with a minimum feature size of 5 μm (to improve the spatial resolution of measurement) resulted in lithographic problems related to surface roughness of diamond films. We improved the surface roughness to 30 nm by using an ultrahigh nucleation density of 10^{11} cm^{-2}. To transfer such small thermistors on a curved surface, a new 3-D diamond patterning technique is currently under development. This involves writing a diamond seed pattern directly on the curved surface by a computer-controlled nozzle.

REFERENCES

1. W. Schafer, Sensors and Actuators, 17, 27-37 (1989).
2 S. Middelhoek and S. A. Audit, Silicon Sensors, Academic Press, London (1989).
3 T. D. McGee, Principles and Methods of Temperature Measurements, John Wiley & Sons (1988).
4 A. Boyer, E. Cisse, Y. Azzouz and J. P. Cheron, Sensors and Actuators, A, 25-27, 637-640 (1991).
5. D. E. Bahniuk, Machine Design, 111-114, Feb, (1989); W. J. Tompkins and J. G. Webster, Interfacing Sensors to the IBM PC, Prentice Hall, Englewood Cliffs, NJ (1988).
6. T. Nugai and M. Itoh, IEEE Trans. Industry Applications, 26(6), 1139-1143 (1990).
7. C. E. Woodhouse, IEEE Trans. Instrum. and Meas., 39(1), 279-284 (1990).
8. S. A. Obukhov, B. S. Neganov, Y. F. Kiselov, A. N. Chernikov, V. S. Vekshina and N. I. Pepkik and A. N. Popkov, Cryogenics (UK), 31(10), 874-877 (1991).
9. G. B. Rogers and F. A. Raal, Rev. Sci. Inst, 31, 663-664 (1960); U.S. Patent, 3,435,399, 25 March (1969).
10. N. Fujimori and H. Nakahata, New Diamonds, 98-101 (1990).
11. I. Taher, M. Aslam, M. A. Tamor, T. J. Potter, and R. E. Elder, Sensors and Actuators: A., Vol. 45, 35 (1994).
12. M. Aslam, G. S. Yang, and A. Masood, Sensors and Actuators: A., Vol. 45, No. 2, 131 (1994).
13. M. Aslam and D. Schulz, Proc. Int. Conf. Solid State Sensors & Actuators (Transducers 95), Stockhom, Sweden, 1995.
14. M. W. Geis, N. N. Efremow, J. D. Woodhouse, M. D. Aleese, M. Marchywka, D. G. Socker, and J. F. Hochedez, IEEE Elec. Dev. Lett., 12, 456 (1991).
15. S. Matsumoto, Y. Sato, M. Kamo and N. Setaka, Jpn. J. Appl. Phys., 21, L183 (1982).
16. J. C. Angus and C.C. Hayman, Science, vol. 241, p. 913, (1988).
17. K. Hirabayashi and Y. Taniguchi, Appl. Phys. Lett., 53, 19 (1988); J. S. Ma, H. Kawarada, T. Yonehara, J. Suzuki, J. Wei, Y. Yokota, and A. Hiraki, Appl. Phys. Lett., 55, 1071 (1989).
18. A. R. Kirkpatric, B. W. Ward, and N. P. Economou, J. Vac. Sci. Technol., 7, 60 (1989).
19. J. L. Davison, C. Ellis and R. Ramesham, J. Electron. Mater., 18, 711-715 (1985).
20. S. A. Grot, C. W. Hatfield, G. S. Gildenblat, A. R. Badzian, and T. Badzian, IEEE Electron. Dev. Lett. (1991).
21. A. Masood, M. Aslam, M.A. Tamor, T.J Potter, J. Electrochem. Soc., 138, L67(1991).

22. G. S. Yang and M. Aslam, Appl. Phys. Lett. 66(3), (1995).

23. G. S. Yang, M. Aslam, M. J. Ulczynski, and D. K. Reinhard, Proc. of 4th ICNDST, Kobe, Japan (1994).

24. H. Shiomi, H. Nakahata, T. Imai, Y. Nishibayashi and N. Fujimori, Jpn. J. Appl. Phys., 28(5), 758-762 (1989).

25. M. W. Geis, IEEE Proceedings, 79(5), 669-675 (1991).

26. F. Fang, C. A. Hewett, M. G. Fernandes and S. S. Lau, IEEE Trans. Electron Devices, 36, 1783-1786 (1989).

27. A. T. Collins, E. C. Lightowlers, and A. W. S. Williams, Diamond Res., pp. 19-22, (Suppl. Ind. Diamond Rev.) (1970).

28. G. S. Gildenblat, S. A. Grot, C. W. Hatfield, and A. R. Badzian, IEEE Electron. Dev. Lett., EDL-12 (2), 37 - 39 (1991).; G. S. Gildenblat, IEEE Electron. Dev. Lett., EDL-11, 371-372, Sep. (1990); H. Shiomi, Y. N. Yashi, and N. Fujimori, Jpn. J. Appl. Phys., 28, L2153-2154 (1989).

29. J. F. Prins, Appl. Phys. Lett., 41(10), 950-952 (1982).

30. J. E. Field, The Properties of Diamond, Academic Press, (1971).

31. S. A. Grot, G. S. Gildenblat, C. W. Hatfield, C. R. Wronski, A. R. Badzian, T. Badzian and R. Messier, IEEE Electron Dev. Lett., EDL-11(2), 100-102 (1990).

32. M. I. Landstrass and K. V. Ravi, Appl. Phys. Lett., 55 (14), 1391 - 1393 (1989); L. S. Pan, D. R. Kania, S. Han, J. W. Ager III, M. Landstrass, O. L. Landen and P. Pianetta, Science, 255, 830-833 (1992).

33. H. Chiemi and Y. Sato, New Diamond, 6, 32 (1990).

34. R. J. Vidal, Cornell Aeronautical Laboratory Buffalo NY rept., AD-917-A-1 (1956).

35. G. S. Yang, M. Asalm, K. P. Kuo, D. K. Reinhard, and J. Asmussem, J. Vac. Sci. and Technol., May/June, (1995).

36. H. W. Ko, S. E. Hsu, S. J. Yang, M. S. Tsai, and Y. H. Lee, Diamond and Related Materials, 2, 694 (1993).

37. L. J. Van der Pauw, Phillips Res. Repts., 13, 1-9 (1958).

38. M. Aslam, Pending Patent, Michigan State University, 1994.